



## Influence of the Deposition Temperature on the c-Si Surface Passivation by Al<sub>2</sub>O<sub>3</sub> Films Synthesized by ALD and PECVD

G. Dingemans,<sup>z</sup> M. C. M. van de Sanden, and W. M. M. Kessels\*

Department of Applied Physics, Eindhoven University of Technology, 5600 MB Eindhoven, The Netherlands

The material properties and c-Si surface passivation have been investigated for Al<sub>2</sub>O<sub>3</sub> films deposited using thermal and plasma atomic layer deposition (ALD) and plasma-enhanced chemical vapor deposition (PECVD) for temperatures ( $T_{\text{dep}}$ ) between 25 and 400°C. Optimal surface passivation by ALD Al<sub>2</sub>O<sub>3</sub> was achieved at  $T_{\text{dep}} = 150\text{--}250^\circ\text{C}$  with  $S_{\text{eff}} < 3\text{ cm/s}$  for  $\sim 2\text{ }\Omega\text{ cm}$  p-type c-Si. PECVD Al<sub>2</sub>O<sub>3</sub> provided a comparable high level of passivation for  $T_{\text{dep}} = 150\text{--}300^\circ\text{C}$  and contained a high fixed negative charge density of  $\sim 6 \times 10^{12}\text{ cm}^{-2}$ . Outstanding surface passivation performance was therefore obtained for thermal ALD, plasma ALD, and PECVD for a relatively wide range of Al<sub>2</sub>O<sub>3</sub> material properties.

© 2009 The Electrochemical Society. [DOI: 10.1149/1.3276040] All rights reserved.

Manuscript submitted November 10, 2009; revised manuscript received November 30, 2009. Published December 29, 2009.

Al<sub>2</sub>O<sub>3</sub> recently emerged as an effective material for the passivation of crystalline silicon (c-Si) surfaces, enabling ultralow surface recombination velocities ( $S_{\text{eff}}$ ) on p-, n-, and p<sup>+</sup>-type c-Si<sup>1,2</sup> leading to enhanced solar cell efficiencies.<sup>3-5</sup> A combination of chemical passivation (i.e., the reduction of interface defects) and field-effect passivation (i.e., electrostatic shielding of minority charge carriers) provided by a large amount of fixed negative charges located at the c-Si/Al<sub>2</sub>O<sub>3</sub> interface is key to the high level of surface passivation achieved. To date, the Al<sub>2</sub>O<sub>3</sub> surface passivation films were mostly synthesized by plasma and thermal atomic layer deposition (ALD) at a substrate temperature of  $\sim 200^\circ\text{C}$ .<sup>1-8</sup> Very recently, it has been shown that other techniques, such as sputtering and plasma-enhanced chemical vapor deposition (PECVD),<sup>9-11</sup> can also be used to deposit Al<sub>2</sub>O<sub>3</sub> surface passivation films. These alternative deposition techniques allow for higher growth rates but generally do not surpass ALD in terms of material and surface passivation quality.

In this article, the influence of the substrate temperature ( $T_{\text{dep}}$ ) during deposition on the Al<sub>2</sub>O<sub>3</sub> material properties and the surface passivation performance is addressed for Al<sub>2</sub>O<sub>3</sub> films deposited at temperatures in the range of  $T_{\text{dep}} = 25\text{--}400^\circ\text{C}$  for thermal and plasma ALD and PECVD. We report that PECVD can be used to deposit Al<sub>2</sub>O<sub>3</sub> films that provide a similar level of surface passivation as ALD Al<sub>2</sub>O<sub>3</sub> while enabling higher deposition rates. By corona charging experiments, the presence of a high fixed negative charge density in the PECVD Al<sub>2</sub>O<sub>3</sub> films is demonstrated.

### Experimental

A direct comparison between thermal ALD and plasma ALD was enabled by employing both methods in an Oxford Instruments OpAL ALD reactor (operating pressure  $\sim 170\text{ mTorr}$ ) and in a second reactor, the Oxford Instruments FlexAL (operating pressure  $\sim 15\text{ mTorr}$ ). For both ALD methods, trimethylaluminum [Al(CH<sub>3</sub>)<sub>3</sub>] was used as the Al precursor in the first half cycle of the ALD process. During the second half cycle, either H<sub>2</sub>O or an O<sub>2</sub> plasma was used for thermal and plasma ALD, respectively.<sup>7</sup> Cycle and purge times were optimized to reach a truly self-limiting ALD process at every  $T_{\text{dep}}$ . The PECVD process employed a continuous remote O<sub>2</sub>/Ar plasma and Al(CH<sub>3</sub>)<sub>3</sub> as the Al precursor. Unlike ALD, the deposition rate for PECVD scaled with the Al(CH<sub>3</sub>)<sub>3</sub> flow that was introduced into the reactor. The refractive index (at a photon energy of 2 eV) and growth rate were determined by in situ spectroscopic ellipsometry, the atomic Al and O densities were determined by Rutherford backscattering spectroscopy, and the atomic hydrogen density was determined by elastic recoil detection. To

evaluate the level of surface passivation, low resistivity p- and n-type  $\sim 275\text{ }\mu\text{m}$  thick float zone (100) c-Si wafers were coated on both sides with Al<sub>2</sub>O<sub>3</sub> with a thickness of  $\sim 30\text{ nm}$ . Before deposition, the wafers were treated with diluted HF (1% in deionized H<sub>2</sub>O). The surface passivation was evaluated in the as-deposited state and after a 10 min postdeposition anneal at  $400^\circ\text{C}$  in a N<sub>2</sub> environment.<sup>7</sup> The upper limit of the surface recombination velocity ( $S_{\text{eff,max}}$ ) was determined from the effective lifetime ( $\tau_{\text{eff}}$ ), as measured with photoconductance (Sinton WCT 100) at an injection level of  $10^{15}\text{ cm}^{-3}$  by assuming an infinite bulk lifetime.<sup>2</sup>

### Results and Discussion

The results regarding the substrate temperature variation are shown in Fig. 1-3. The growth rate, refractive index, and surface passivation performance were evaluated for plasma and thermal ALD in Fig. 1 and for PECVD in Fig. 2. The mass density, atomic O/Al ratio, and hydrogen concentration for corresponding Al<sub>2</sub>O<sub>3</sub> films are displayed in Fig. 3.

The results for the growth-per-cycle (GPC) as a function of  $T_{\text{dep}}$  for plasma and thermal ALD (Fig. 1a) agree well for the OpAL and the FlexAL reactors. The higher GPC for plasma ALD compared to thermal ALD, which is observed over the full temperature range but particularly pronounced at low temperatures, has been ascribed to a more efficient surface oxidation by plasma-generated O radicals compared to thermally activated oxidation by H<sub>2</sub>O.<sup>12</sup> The decrease in GPC with increasing  $T_{\text{dep}}$  can be mainly attributed to a decreasing density of OH surface groups due to dehydroxylation reactions.<sup>12,13</sup> The refractive index (Fig. 1b) increases with deposition temperature, which is directly linked to material densification, as displayed in Fig. 3a. The mass density of the films increased with  $T_{\text{dep}}$ , saturating at  $3.2 \pm 0.2\text{ g/cm}^3$  at a high temperature.

In Fig. 2a and b, the deposition rate and refractive index as a function of substrate temperature are shown for the PECVD process. The values were measured at a fixed location on the various wafers, as a variation in thickness, and refractive index was observed for the PECVD samples due to the nonuniformity of the film caused by the deposition technique. The refractive index and mass density (Fig. 3a) increased with  $T_{\text{dep}}$ , similar to the ALD case. The refractive index values for PECVD Al<sub>2</sub>O<sub>3</sub> are lower than the ones obtained for ALD at the same  $T_{\text{dep}}$ . The deposition rate,  $R_{\text{dep}}$ , decreased strongly with increasing  $T_{\text{dep}}$ , saturating at  $\sim 5\text{ nm/min}$  for  $T_{\text{dep}} > 200^\circ\text{C}$ . The higher  $R_{\text{dep}}$  at low temperature can be partly attributed to a lower mass density linked to a higher density of hydrogen (mainly incorporated as OH groups) and carbon-related impurities in the films, as revealed by IR absorption analyses. Furthermore, the general trend of  $R_{\text{dep}}$  as a function of  $T_{\text{dep}}$  is an indication of a growth process controlled by the adsorption of surface species, as also pre-

\* Electrochemical Society Active Member.

<sup>z</sup> E-mail: g.dingemans@tue.nl

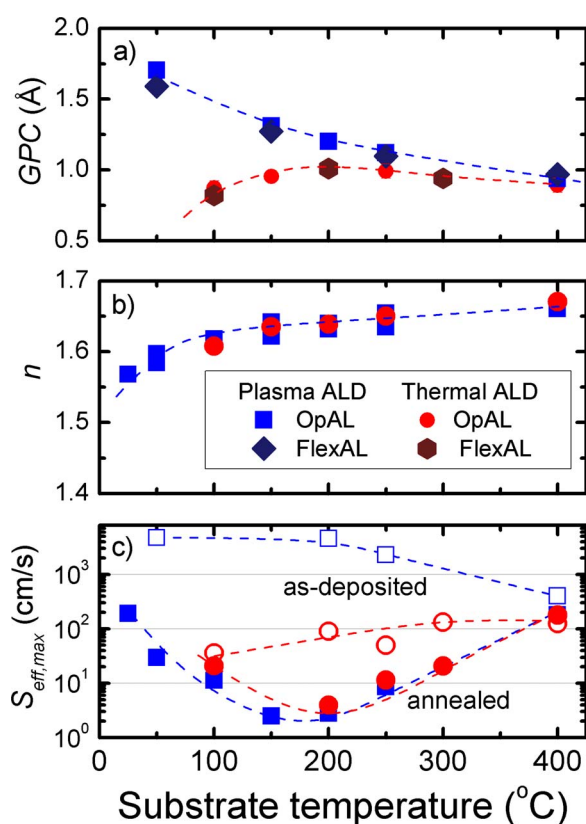


**Figure 1.** (Color online) (a) GPC, (b) refractive index,  $n$ , and (c) maximum surface recombination velocity,  $S_{eff,max}$ , as a function of substrate temperature for plasma and thermal ALD. The data in (c) correspond to  $\text{Al}_2\text{O}_3$  deposited on  $\sim 2 \Omega \text{ cm}$  p-type c-Si in the OpAL reactor. Open symbols represent as-deposited  $\text{Al}_2\text{O}_3$  films and closed symbols films after annealing at 400 °C. Lines serve as a guide for the eyes.

viously reported for the PECVD of  $\text{SiO}_2$ .<sup>14</sup> Dehydroxylation reactions could also play a role, but a more in-depth research is necessary to further elucidate the growth mechanism.

For all three deposition methods, the material densification with increasing  $T_{dep}$  can be partly explained by the decreasing hydrogen concentration as evidenced by Fig. 3c. For the same  $T_{dep}$ , the hydrogen concentrations of the PECVD  $\text{Al}_2\text{O}_3$  films were significantly higher than those for the ALD  $\text{Al}_2\text{O}_3$  films. The O/Al ratio decreased with increasing  $T_{dep}$ , as displayed in Fig. 3b, and (nearly) stoichiometric  $\text{Al}_2\text{O}_3$  films, with O/Al ratios close to 1.5, were obtained at  $T_{dep} > 200^\circ\text{C}$ .

The level of c-Si surface passivation by ALD-synthesized  $\text{Al}_2\text{O}_3$  is evaluated in Fig. 1c. The results demonstrate that thermal ALD  $\text{Al}_2\text{O}_3$  provides a higher level of surface passivation in the as-deposited state (with lowest  $S_{eff} < 35 \text{ cm/s}$ ) than plasma ALD  $\text{Al}_2\text{O}_3$ .<sup>7</sup> It is observed that the as-deposited passivation quality increases with  $T_{dep}$  for the plasma ALD, whereas a small decrease with increasing  $T_{dep}$  is observed for the thermal ALD. After annealing, the surface passivation quality improved significantly,<sup>7,15</sup> with the best passivation performance obtained at  $T_{dep} = 150\text{--}250^\circ\text{C}$  for both ALD methods. Values of  $S_{eff,max}$  down to  $\sim 3 \text{ cm/s}$  are reached for  $\sim 2 \Omega \text{ cm}$  p-type c-Si by both plasma and thermal ALD.

The trend observed for the passivation quality of the as-deposited PECVD  $\text{Al}_2\text{O}_3$ , shown in Fig. 2c, is similar to the one for plasma ALD  $\text{Al}_2\text{O}_3$ . Annealing also improved the passivation properties of the PECVD  $\text{Al}_2\text{O}_3$  films. The annealed films afforded a high level of surface passivation with  $S_{eff} < 10 \text{ cm/s}$  for  $T_{dep} = 150\text{--}300^\circ\text{C}$ . In addition to the data shown in Fig. 2c, exceptionally low  $S_{eff}$  values were obtained at  $T_{dep} = 200^\circ\text{C}$ , for example,  $S_{eff} < 2.9 \text{ cm/s}$  ( $\tau_{eff}$

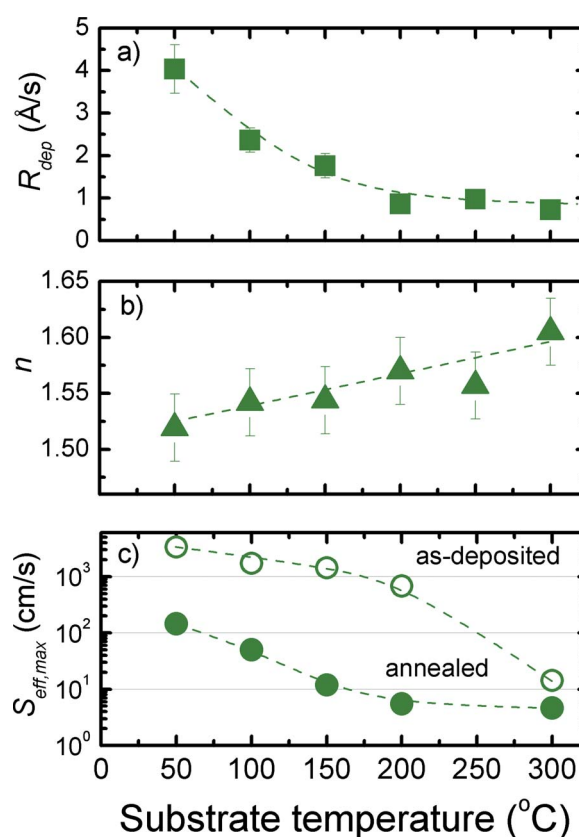


**Figure 2.** (Color online) (a) Deposition rate,  $R_{dep}$ , (b) refractive index,  $n$ , and (c) maximum surface recombination velocity,  $S_{eff,max}$ , on  $\sim 2 \Omega \text{ cm}$  p-type c-Si as a function of substrate temperature for PECVD  $\text{Al}_2\text{O}_3$ . Open symbols represent as-deposited  $\text{Al}_2\text{O}_3$  films and closed symbols films after annealing at 400 °C. Lines serve as a guide for the eyes.

$= 4.7 \text{ ms}$ ) and  $S_{eff} < 0.8 \text{ cm/s}$  ( $\tau_{eff} = 18 \text{ ms}$ ) on  $2.2 \Omega \text{ cm}$  p-type and  $3.5 \Omega \text{ cm}$  n-type c-Si, respectively; and also  $S_{eff} < 14 \text{ cm/s}$  ( $\tau_{eff} = 1 \text{ ms}$ ) on  $1 \Omega \text{ cm}$  p-type c-Si. The corresponding injection-level-dependent lifetime curves are displayed in Fig. 4. These results were obtained with a deposition rate of  $\sim 5 \text{ nm/min}$ . Significantly higher deposition rates of  $> 30 \text{ nm/min}$  were also feasible while maintaining a good level of surface passivation, as demonstrated by  $S_{eff} < 14 \text{ cm/s}$  on  $3.5 \Omega \text{ cm}$  n-type c-Si. For comparison, under the present conditions the maximum deposition rate for ALD was  $\sim 1.8 \text{ nm/min}$  at  $T_{dep} = 200^\circ\text{C}$ .

The improvement of the passivation properties of the as-deposited plasma ALD and PECVD  $\text{Al}_2\text{O}_3$  films with increasing  $T_{dep}$  can be explained by an in situ anneal effect at high temperatures. The interfacial oxide ( $\text{SiO}_x$ ) that forms between c-Si and  $\text{Al}_2\text{O}_3$  is thought to play an essential role in the surface passivation properties of  $\text{Al}_2\text{O}_3$ .<sup>15</sup> The interface quality and related surface passivation properties improve during plasma ALD and PECVD at high temperatures, which is similar to the effect observed during the post-deposition anneal.<sup>7,15</sup> For thermal ALD, an in situ anneal effect was not observed, and  $S_{eff,max}$  for the as-deposited films even slightly increased with increasing  $T_{dep}$ . Apparently, lower temperatures led to improved interface properties for  $\text{Al}_2\text{O}_3$  deposited by thermal ALD.

The  $\text{Al}_2\text{O}_3$  material properties are expected to affect both the chemical and field-effect contributions to the surface passivation performance of the films. The fixed negative charge density,  $Q_f$ , that increases drastically during annealing,<sup>15,16</sup> induces the field-effect passivation and is expected to be closely related to the  $\text{Al}_2\text{O}_3$  structural properties near the interface.<sup>15</sup> As shown in Fig. 5, we have also verified the presence of a high negative  $Q_f$  of  $(6.5 \pm 1)$

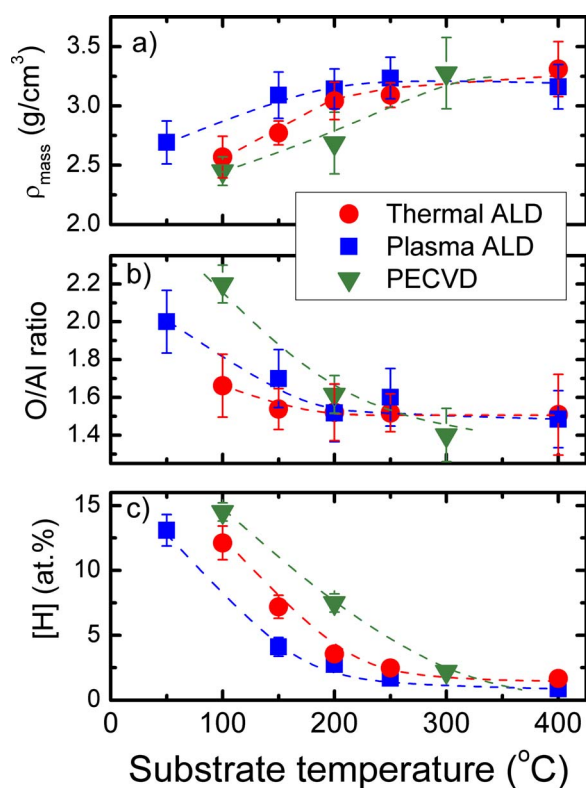


**Figure 3.** (Color online) (a) Mass density,  $\rho_{\text{mass}}$ , (b) O/Al ratio, and (c) the H concentration, [H], determined as a function of substrate temperature for as-deposited films. Data are given for plasma and thermal ALD  $\text{Al}_2\text{O}_3$  films deposited in the OpAL reactor and PECVD  $\text{Al}_2\text{O}_3$  films. Lines serve as a guide for the eyes.

$\times 10^{12} \text{ cm}^{-2}$  for PECVD  $\text{Al}_2\text{O}_3$  deposited at  $T_{\text{dep}} = 200^\circ\text{C}$  after annealing.  $Q_f$  was determined by depositing positive corona charges on a passivated c-Si wafer using a similar approach, as described in Ref. 2. A sharp drop of the level of surface passivation (increase in  $S_{\text{eff,max}}$ ) was observed at the point where the amount of negative fixed charge in the  $\text{Al}_2\text{O}_3$  was exactly balanced by positive corona charges. In the same way, a negative  $Q_f$  of  $(5 \pm 1) \times 10^{12} \text{ cm}^{-2}$  for plasma ALD  $\text{Al}_2\text{O}_3$  was determined. These  $Q_f$  values for plasma ALD and PECVD  $\text{Al}_2\text{O}_3$  are higher than the negative  $Q_f$  values reported for microwave PECVD ( $Q_f \approx 2 \times 10^{12} \text{ cm}^{-2}$ )<sup>11</sup> and

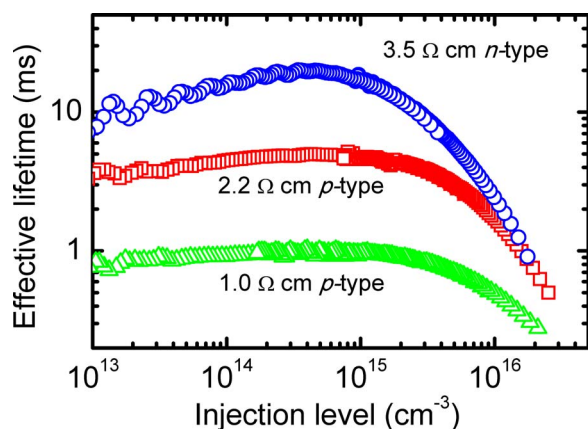


**Figure 4.** (Color online) Injection-level-dependent effective lifetime for n- and p-type c-Si wafers of various resistivities passivated by PECVD  $\text{Al}_2\text{O}_3$  with  $T_{\text{dep}} = 200^\circ\text{C}$  after annealing.

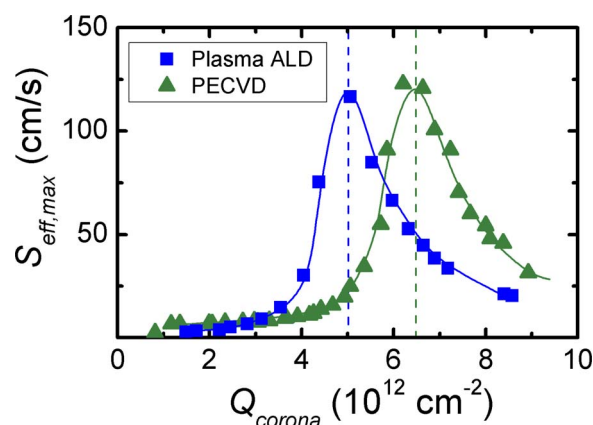


**Figure 5.** (Color online) Maximum surface recombination velocity  $S_{\text{eff,max}}$  as a function of the positive corona charge density  $Q_{\text{corona}}$  deposited on  $\text{Al}_2\text{O}_3$  films synthesized by plasma ALD and PECVD ( $T_{\text{dep}} = 200^\circ\text{C}$ ) after annealing. As substrates,  $3.5 \Omega \text{ cm}$  n-type c-Si wafers were used.

sputtered  $\text{Al}_2\text{O}_3$  ( $Q_f \approx 3 \times 10^{12} \text{ cm}^{-2}$ ).<sup>9</sup> Our measured  $Q_f$  values are within the range of the previously reported values of negative  $Q_f$  between  $5 \times 10^{12}$  and  $13 \times 10^{12} \text{ cm}^{-2}$  for plasma ALD  $\text{Al}_2\text{O}_3$ .<sup>2,15,16</sup> For thermal ALD  $\text{Al}_2\text{O}_3$  preliminary data suggest that after annealing the negative  $Q_f$  values are significantly lower.

Comparing the material properties with the passivation performance of  $\text{Al}_2\text{O}_3$  films, it is apparent that conventional measures for high material quality, such as a high refractive index and mass density, stoichiometry (O/Al ratio  $\sim 1.5$ ), and low impurity content, do not directly reflect the passivation performance. In fact, a high level of surface passivation was obtained for a relatively wide range of  $\text{Al}_2\text{O}_3$  material properties, such as a refractive index and hydrogen concentration in the range of 1.55–1.65 and 2–7.5 atom %, respectively. This observation is consistent with the expectation that, ultimately, after annealing, the c-Si/ $\text{Al}_2\text{O}_3$  interface properties determine the level of surface passivation and that the  $\text{Al}_2\text{O}_3$  bulk material properties may deviate from those close to the c-Si interface.<sup>17,18</sup> During postdeposition annealing, structural modification of the material bulk and interface takes place,<sup>2,8,18</sup> which improves the surface passivation of c-Si. These structural rearrangements, in conjunction with the importance of the interface properties, might relax the requirements on the  $\text{Al}_2\text{O}_3$  bulk material properties significantly.

## Conclusion

We have studied the influence of the substrate temperature on the material properties and the surface passivation performance of  $\text{Al}_2\text{O}_3$  films synthesized by plasma and thermal ALD and PECVD. The  $\text{Al}_2\text{O}_3$  material properties, such as mass density and hydrogen content, were dependent on the deposition technique used, but the resulting surface passivation performance was excellent for plasma and thermal ALD  $\text{Al}_2\text{O}_3$  at  $T_{\text{dep}} = 150$ – $250^\circ\text{C}$  and for PECVD  $\text{Al}_2\text{O}_3$  at  $T_{\text{dep}} = 150$ – $300^\circ\text{C}$ . Consequently, a principal result of this work is that we have demonstrated that PECVD can be used to deposit high quality  $\text{Al}_2\text{O}_3$  films, resulting in exceptionally low surface recombination velocities and containing a high fixed negative charge density of  $\sim 6 \times 10^{12} \text{ cm}^{-2}$ . The deposition method of choice for  $\text{Al}_2\text{O}_3$  therefore depends largely upon the extent to which other relevant factors (such as deposition uniformity, conformality, throughput, and scalability) play a role in the envisaged application of  $\text{Al}_2\text{O}_3$ .

## Acknowledgments

We thank Dr. R. Seguin and Dr. P. Engelhart (Q-Cells) for fruitful discussions. Dr. V. Verlaan, Dr. M. Mandoc, L. van den Elzen, C. van Helvoirt, and M. Adams (TU/e) are acknowledged for assisting

with the experiments. This work was supported by the German Ministry for the Environment, Nature Conservation and Nuclear Safety (BMU) under contract no. 0325150 ("ALADIN").

Eindhoven University of Technology assisted in meeting the publication costs of this article.

### References

1. B. Hoex, J. Schmidt, R. Bock, P. P. Altermatt, M. C. M. van de Sanden, and W. M. M. Kessels, *Appl. Phys. Lett.*, **91**, 112107 (2007).
2. B. Hoex, J. Schmidt, P. Pohl, M. C. M. van de Sanden, and W. M. M. Kessels, *J. Appl. Phys.*, **104**, 044903 (2008).
3. J. Benick, B. Hoex, M. C. M. van de Sanden, W. M. M. Kessels, O. Schultz, and S. W. Glunz, *Appl. Phys. Lett.*, **92**, 253504 (2008).
4. J. Schmidt, A. Merkle, R. Brendel, B. Hoex, M. C. M. van de Sanden, and W. M. M. Kessels, *Prog. Photovoltaics*, **16**, 461 (2008).
5. W. C. Sun, W. L. Chang, C. H. Chen, C. H. Du, T. Y. Wang, T. Wang, and C. W. Lana, *Electrochem. Solid-State Lett.*, **12**, H388 (2009).
6. G. Agostinelli, A. Delabie, P. Vitanov, Z. Alexieva, H. F. W. Dekkers, S. De Wolf, and G. Beaucarne, *Sol. Energy Mater. Sol. Cells*, **90**, 3438 (2006).
7. G. Dingemans, R. Seguin, P. Engelhart, M. C. M. van de Sanden, and W. M. M. Kessels, *Phys. Status Solidi (RRL)*, **4**, 10 (2010).
8. G. Dingemans, P. Engelhart, R. Seguin, F. Einsele, B. Hoex, M. C. M. van de Sanden, and W. M. M. Kessels, *J. Appl. Phys.*, **106**, 114907 (2009).
9. T.-T. Li and A. Cuevas, *Phys. Status Solidi (RRL)*, **3**, 160 (2009).
10. S. Miyajima, J. Irikawa, A. Yamada, and M. Konagai, in *23rd European Photovoltaic Solar Energy Conference*, WIP Renewable Energies, Valencia (2008).
11. P. Saint-Cast, D. Kania, M. Hofmann, J. Benick, J. Rentsch, and R. Preu, *Appl. Phys. Lett.*, **95**, 151502 (2009).
12. E. Langereis, J. Keijmel, M. C. M. van de Sanden, and W. M. M. Kessels, *Appl. Phys. Lett.*, **92**, 231904 (2008).
13. R. L. Puurunen, *J. Appl. Phys.*, **97**, 121301 (2005).
14. I. T. Emesh, G. D'Asti, J. S. Mercier, and P. Leung, *J. Electrochem. Soc.*, **136**, 3404 (1989).
15. B. Hoex, J. J. H. Gielis, M. C. M. van de Sanden, and W. M. M. Kessels, *J. Appl. Phys.*, **104**, 113703 (2008).
16. J. J. H. Gielis, B. Hoex, M. C. M. van de Sanden, and W. M. M. Kessels, *J. Appl. Phys.*, **104**, 073701 (2008).
17. K. Kimoto, Y. Matsui, T. Nabatame, T. Yasuda, T. Mizoguchi, I. Tanaka, and A. Toriumi, *Appl. Phys. Lett.*, **83**, 4306 (2003).
18. V. Verlaan, L. R. J. G. van den Elzen, G. Dingemans, M. C. M. van de Sanden, and W. M. M. Kessels, *Phys. Status Solidi A*, In press.